1996

Analysis of Transient Hydrogen Uptake by Metal Alloy Particles

Wenlin Zhang
Texas A & M University - College Station

Supramaniam Srinivasan
University of South Carolina - Columbia

Harry J. Ploehn
University of South Carolina - Columbia, ploehn@cec.sc.edu

Publication Info

Journal of the Electrochemical Society, 1996, pages 4039-4047.

Publisher's link: http://dx.doi.org/10.1149/1.1837333
DOI: 10.1149/1.1837333

10. J. S. Gill, L. M. Callow, and J. D. Scantlebury, *Corrosion,* **39,** 61 (1983).
11. S. Sathiyanarayanan and K. Balakrishnan, *Brit. Corros. J.,* **29,** 152 (1994).
12. L. Mészáros and J. Dévay, *Acta Chim. Hung.,* **129,** 79 (1992).
13. L. Mészáros and J. Dévay, *ibid.,* **129,** 83 (1992).
14. M. Sluyters-Rehbach and J. H. Sluyters, in *Electroanalytical Chemistry,* Vol. 4, A. J. Bard, Editor, p.1, Marcel Dekker, Inc., New York (1970).
15. S. K. Rangarajan, *J. Electranal. Chem.* **1,** 396 (1959/60).
16. A. J. Bard and L. R. Faulkner, *Electrochemical Methods, Fundamentals and Applications,* p. 326, John Wiley & Sons, Inc., New York (1980).
17. M. Abramowitz and I. A. Stegun, *Handbook of Mathematical Functions,* Dover Publications, New York (1968).
18. W. H. Beyer, *CRC Standard Mathematical Tables,* CRC Press, Boca Raton, FL (1981).
19. H. W. William, S. A. Teukolsky, W. T. Vetterling, and B. P. Flamery, *Numerical Recipes,* p. 340, 2nd ed., Cambridge University Press (1992).
20. *MathCad 4.0 User's Guide,* 4th ed., Cambridge, USA (1993).
21. J. O' M. Bockris and A. K. N. Reddy, *Modern Electrochemistry,* p. 737, Plenum Press, New York (1970).
22. A. J. Bard and L. R. Faulkner, *Electrochemical Methods, Fundamentals and Applications,* p. 511, John Wiley & Sons, Inc. New York (1980).
23. J. A. L. Dobbelaar, Ph.D. Thesis, University of Delft, Netherlands (1990).
24. J. A. L. Dobbelaar and J. H. W. de Wit, *This Journal,* **137,** 2038 (1990).
25. *LabVIEW for Windows Version 3.0,* National Instruments Corporation (1993).
26. G. W. Johnson, *LabView, Graphical Programming: Practical Application in Instrumentation and Control,* McGraw Hill, New York (1994).
27. L. P. B. M. Janssen and M. M. C. G. Warmoeskerken, *Transport Phenomena Data Companion,* DUM, Delft (1987).
28. V. Jovancicevic and J. O'M. Bockris, *This Journal,* **33,** 1797 (1986).
29. J. O' M. Bockris and S. U. M. Khan, *Surface Electrochemistry, A Molecular Level Approach,* p. 333, Plenum Press, New York (1993).
30. K. Jüttner, W. J. Lorenz, M. W. Kendig, and F. Mansfeld, *This Journal,* **135,** 332 (1988).
31. K. Jüttner, K. Manandhar, U. Seifert-Kraus, W. J. Lorenz, and E. Schmidt, *Werkst. Korros.* **37,** 377 (1986).

Analysis of Transient Hydrogen Uptake by Metal Alloy Particles

Wenlin Zhang,*[a,c] Supramaniam Srinivasan,[,b] and Harry J. Ploehn[b]**

[a]*Center for Electrochemical Systems and Hydrogen Research, Texas Engineering Experiment Station, Texas A&M University System, College Station, Texas 77843-3402, USA*
[b]*Department of Chemical Engineering, University of South Carolina, Swearingen Engineering Center, Columbia, South Carolina 29208, USA*

ABSTRACT

This paper describes a new approach to solving the equations comprising the shrinking core model for diffusion and reaction of a chemical species in a solid spherical particle. The reactant adsorbs on the particle surface, diffuses into the particle's interior, and reacts with the particle to form a solid product. The shrinking core model assumes a fast reaction rate compared to reactant diffusion so that the reaction is localized in the interfacial zone between the unreacted solid core and the surrounding shell of reacted product. Analytical solutions of the governing conservation equations usually invoke the pseudo-steady state (PSS) approximation which neglects the transient mass accumulation and diffusion-induced convection terms in the continuity equation for the diffusing reactant. However, small particle radii and slow reactant diffusion cast doubt on the validity of the PSS approximation. Dimensional analysis reveals an approximation that is less restrictive than PSS, yet enables a semi-analytical solution for the diffusing reactant distribution and interface velocity. For sufficiently large values of the surface mass fraction of the diffusing reactant, the PSS approximation leads to serious errors in the time dependence of the interface position and fractional conversion. However, our estimate of the surface mass fraction of hydrogen in $LaNi_5$ particles suggests the validity of the PSS approximation for hydriding of metal alloy particles. The shrinking core model thus enables an estimate of hydrogen diffusivity in metal alloy particles.

Introduction

Several rare earth intermetallic compounds of the general composition AB_5 can absorb and release large amounts of hydrogen (H) and thus have potential utility for H storage. For example, various forms of $LaNi_5$ and its alloys have been extensively investigated and used in practical applications.[1,2] Improvements in performance can be achieved by partial substitution of certain elements for either La or Ni in $LaNi_5$.[3] Fundamental understanding of hydriding mechanisms and H transport are leading to better mathematical models that can help guide efforts to synthesize new substituted metal alloys.

The kinetics of the hydriding process have been investigated extensively.[4-8] The hydriding process begins with the entry of H at the surface of the metal alloy particle, either from the gas phase or electrochemically from the liquid phase. Gas-phase and electrochemical hydriding processes differ in their initial step. In the gas-phase hydriding process, the first step is the dissociative adsorption of a hydrogen molecule

$$H_2(g) + 2M \rightleftarrows 2MH_{ads} \quad [1]$$

where 2M represents two neighboring adsorption sites on the alloy surface. In the electrochemical hybriding process, an external circuit supplies electrons to the alloy particles. Hydrogen atoms adsorb in a charge-transfer step

$$H_2O + M + e^- \rightleftarrows MH_{ads} + OH^- \quad [2]$$

followed by subsequent processes that may include electrochemical recombination or other "parasitic" phenomena as well as H diffusion into the particle. Here, we assume that the subsequent hydriding process in the interior of the particle is the same regardless of whether the H enters from the gas phase or from an electrolyte solution.

* Electrochemical Society Student Member.
** Electrochemical Society Active Member.
[c] Present address: Schlumberger Perforating and Testing Center, Rosharon, Texas 77583-1590.

Hydriding of the interior of the metal alloy begins with rapid diffusion of a small amount of H through microcracks or pores into the interior of the metal alloy to produce a dilute solid solution denoted as the α-phase (Fig. 1). Experiments have shown that this process does occur and is rapid,[8] but the resultant H mass fraction in the α-phase is quite small and may be neglected. At the same time, transient surface hydriding occurs as absorbed H reacts with the surface layer of metal alloy to form a surface layer of the metal hydride according to

$$x\mathrm{H} + \mathrm{M} \rightleftarrows \mathrm{MH}_x \qquad [3]$$

The product metal hydride is denoted as the β-phase. Recent experiments[3] have characterized the stoichiometric limit for hydriding of $LaNi_5$ and related partially substituted metal alloys. In most cases, a stoichiometric coefficient x near six has been found for these materials. Here, we treat x as a parameter that is constant throughout the β-phase.

If the reaction rate in the α-phase is fast compared to the rate of H transport through the β-phase, then the reaction, Eq. 3, will be limited to an interfacial zone between the α- and β-phases. After the initial transient hydriding of the surface (not considered in this work), the α/β interface and thus the reaction zone move into the interior of the particle. Figure 1 schematically depicts this process. The hydriding reaction in the particle interior creates a concentration gradient that drives H transport through the metal hydride β-phase. When H reaches the α/β interface, it is incorporated in the growing β-phase.

The β-phase thus contains "free" (nonstoichiometric) H moving through the MH_x toward the α/β interface. Although upper limits on the mass fraction of free H in the β-phase have not been established, observations of H uptake indicate[3] that it never becomes very large.

The mechanism of H transport thought the β-phase has not been fully elucidated. Bulk diffusion of H through a network of pores has been ruled out because intermetallic metal hydride materials are, in fact, alloys with crystalline structure and few pores. Instead, H transport in the β-phase is probably similar to a solid-state electron hopping process.[9] Nuclear magnetic resonance studies[10,11] have identified at least two types of motion, including localized short-range motion associated with M–H bond vibrations, and long-range multistep jumps that are primarily responsible for H transport. These results suggest that as H atoms vibrate and hop around in the crystalline hydride, they remain closely associated with the metal atoms. Nevertheless, the stochastic nature of the jumps suggests that the H transport in the β-phase can be modeled as a diffusion process with low effective diffusivity. Values of H diffusivity are critical for assessing metal alloy performance and for battery design.

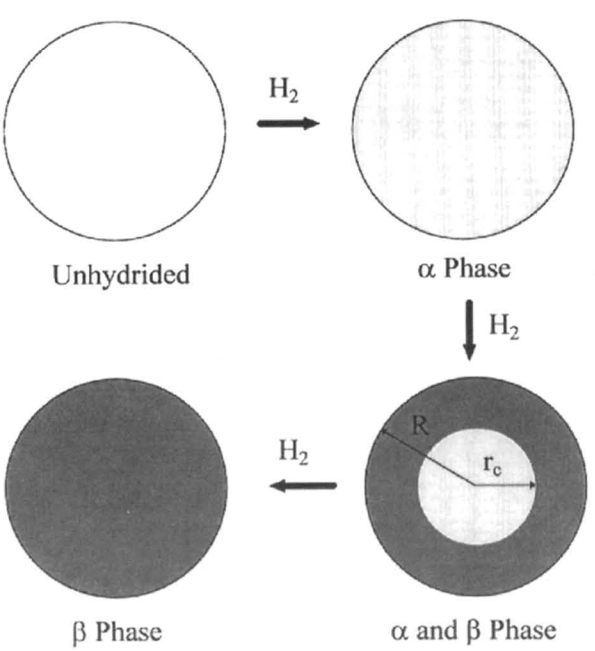

Fig. 1. Schematic representation of the shrinking core model for the uptake of hydrogen by a solid metal alloy particle.

The physical picture of hydriding, as depicted in Fig. 1, can be expressed mathematically as the shrinking core model[12] which has been widely used to describe processes involving diffusion and reaction in spherical particles. Most previous analytical solutions invoked the pseudo-steady state (PSS) approximation[12] which simplifies the mathematics by eliminating the transient and diffusion-induced convection terms in the differential mass balance for the reactant. The validity of the PSS approximation has been tested through comparisons with solutions derived through perturbation methods[13-16] and numerical methods.[17-19] One recent study[18] compared results from an improved perturbation analysis, a moving boundary finite element numerical solution, and the classic PSS solution. However, this model poses a finite reaction rate at the α/β interface which may not be consistent with the neglect of reactant consumption elsewhere in the β-phase. Nonisothermal effects and nonlinear kinetics have also been explored.[19]

Previous studies agree on the validity of the PSS approximation when the concentration of the diffusing reactant is small compared to the solid concentration. Only Lindman and Simonsson[17] recognized that the neglect of diffusion-induced convection might be a cause for concern. None of the previous studies developed rigorous boundary conditions based on jump mass balances.[20] Only Bowen[14] and Bischoff[15] considered the implications of dimensional analysis for assessing the validity of the PSS approximation.

The shrinking core model with the PSS approximation has been used previously to describe H uptake by metal alloy particles.[21,22] However, the validity of the PSS approximation in this application has not been established. Several factors motivate us to address this point. First, dimensional analysis suggests that, because of the low H diffusivity in the β-phase, the transient accumulation term may have a magnitude comparable to that of the diffusion term in the differential mass balance for H. Furthermore, no one has assessed the validity of neglecting the diffusion-induced convection term. Finally, errors introduced by the PSS approximation may prevent accurate determination of H diffusivities from hydriding experiments.

This paper re-examines the shrinking core model as applied to the generic case of transport and reaction of one chemical species ("reactant") inside a solid spherical particle. Differential mass balances for total mass and reactant govern the mass-average velocity and the distribution of reactant in the growing β-phase. Jump balances for total mass, reactant, and solid at the α/β interface combine to relate the α/β interface velocity to the flux of reactant to the interface. Dimensional analysis of the reactant continuity equation (mass balance) shows that the diffusion-induced convection and homogenous reaction terms can be neglected when the α- and β-phases have similar densities and the reaction rate in the β-phase is small.

However, slow reactant diffusion in the β-phase implies that transient accumulation term and the diffusion term in the reactant continuity equation have the same magnitude. This necessitates the development of a solution that is less restrictive than the classic PSS approximation. A semi-analytical "transient" solution of the reactant continuity equation expresses the spatial and temporal variations of the reactant mass fraction and the velocity of the α/β interface. Numerical integration of the latter fixes the spatial position of the α/β interface as a function of time, allowing evaluation of the reactant mass fraction distribution and the fractional conversion. The results obtained from this transient model are compared with those calculated under the PSS approximation, enabling us to assess the validity of the PSS solution under different conditions. Finally, we use the

generic model to consider the particular case of hydrogen uptake by metal alloy particles.

Theoretical Model

Transient shrinking core model.—The generic shrinking core model treats the general case of reactant (H) transported through a spherical shell of reacted product (MH_x) towards the core of unreacted solid (M) at the center. Each internal phase has uniform internal crystalline structure. The core (α-phase) contains only unreacted solid (M). The shell (β-phase) contains reacted product (MH_x) and free reactant (H). Although the species labels suggest hydriding of metal alloys, the model should be viewed as a generic one for reactant uptake via diffusion through and reaction with a solid spherical particle.

Spherical symmetry eliminates all angular velocity components and the dependence of the remaining variables on angular coordinates. The effective reactant diffusivity in the β-phase, D, is assumed to be constant. Likewise, the bulk densities of the α- and β-phases, ρ^α and ρ^β, are approximated as constant but unequal. We also assume that the particles remain at constant temperature.

In spherical coordinates, the continuity equation for phase $i (i = \alpha$ or $\beta)$ reduces to

$$\frac{\partial}{\partial r}(r^2 v_r^i) = 0 \qquad [4]$$

where v_r^i is the mass-average radial velocity at each point in phase i. This equation has the solution

$$v_r^\alpha = 0 \qquad [5]$$

in the α-phase, since the velocity must be finite at $r = 0$. Likewise, for the β-phase, we find

$$r^2 v_r^\beta = C^\beta(t) \qquad [6]$$

indicating that the product $r^2 v_r^\beta$ in the β-phase is at most a function of time.

The α/β interface is located at $r = r_c$. The overall jump mass balance at the α/β interface

$$\text{at } r = r_c \qquad \rho^\beta(v_r^\beta - s) - \rho^a(v_r^a - s) = 0 \qquad [7]$$

can be derived from the general transport theorem for bodies containing a phase interface (Ref. 20, p. 25). Physically, Eq. 7 is a mass conservation statement that relates the normal components of the mass flux on each side of a phase interface moving at a radial velocity s. Using Eq. 5, Eq. 7 simplifies to

$$\text{at } r = r_c \qquad v_r^\beta = \frac{\rho^\beta - \rho^\alpha}{\rho^\beta} s \qquad [8]$$

which relates the mass-average velocity of the β-phase to the α/β interface velocity.

With the constitutive equation for mass flux given by Fick's first law of binary diffusion (Ref. 20, p. 481), the continuity equation for the reactant can be written in terms of mass fractions (ω) as

$$\frac{\partial \omega_H^\beta}{\partial t} + v_r^\beta \frac{\partial \omega_H^\beta}{\partial r} = \frac{D}{r^2}\frac{\partial}{\partial r}\left(r^2 \frac{\partial \omega_H^\beta}{\partial r}\right) - \frac{R_H^\beta}{\rho^\beta} \qquad [9]$$

where R_H^β is the rate of consumption of the reactant in the β-phase due to homogeneous reactions. The initial condition

$$\text{at } t = 0 \text{ for } 0 < r < R \qquad \omega_H^\alpha = \omega_{H0} \approx 0 \qquad [10]$$

follows from the assumption of negligible reactant initially in the particle, and surface boundary condition is

$$\text{for } t > 0,\ r = R \qquad \omega_H^\beta = \omega_{HR} \qquad [11]$$

which is appropriate when we neglect mass transfer resistance at the particle surface. The quantity ω_{HR} represents the mass fraction of free reactant in the solid at the surface, $r = R$.

The jump balance for free reactant at the α/β interface (Ref. 20, p. 451)

$$\text{at } r = r_c \qquad \rho_H^\beta(v_H^\beta - s) - \rho_H^\alpha(v_H^a - s) = -R_H^\sigma \qquad [12]$$

provides the other boundary condition. Physically, Eq. 12 is a mass conservation statement that relates the normal components of the mass flux of the reactant at the moving interface to rate of consumption of reactant at the interface due to chemical reactions. Equation 10 implies that $\rho_H^\alpha \equiv \rho^\alpha \omega_H^\alpha = 0$ so that Eq. 12 becomes

$$\text{at } r = r_c \qquad \rho_H^\beta(v_H^\beta - s) = -R_H^\sigma \qquad [13]$$

The basic premise of the shrinking core model and the neglect of reactant consumption elsewhere in the particle necessitate large values of the reaction rate R_H^σ at the interface. Since both sides of Eq. 13 must be of the same magnitude and ρ_H^β is not large, we require $v_H^\beta >> s$. That is, a fast reaction rate necessitates that the velocity of reactant at the interface must be greater than the velocity of the interface itself. Together with the definition of the mass flux

$$n_H^\beta \equiv \rho_H^\beta v_H^\beta \qquad [14]$$

Eq. 13 becomes

$$\text{at } r = r_c \qquad n_H^\beta = -R_H^\sigma \qquad [15]$$

which, in physical terms, states that the rate of consumption of reactant at the α/β interface equals the reactant mass flux to the interface.

The jump mass balance for unreacted solid (M) at the α/β interface, analogous to Eq. 12, reduces to

$$\text{at } r = r_c \qquad s = -\frac{R_M^\sigma}{\rho_M^\alpha} \qquad [16]$$

after assuming that $v_M^a = 0$ (motionless solid in the α-phase) and $\rho_M^b = 0$ (no unreacted solid in the β-phase). We assume that stoichiometry of the reaction requires the consumption of 1 mole of solid and x moles of reactant for each mole of product produced. Thus

$$r_M^\sigma = \frac{M_M}{xM_H} R_H^\sigma \qquad [17]$$

relates the consumption rates of reactant and solid. Fick's first law of binary diffusion becomes

$$n_H^\beta = -\frac{\rho^\beta D}{(1 - \omega_H^\beta)}\frac{\partial \omega_H^\beta}{\partial r} \approx -\rho^\beta D \frac{\partial \omega_H^\beta}{\partial r} \qquad [18]$$

if we assume zero mass flux of product in the β-phase and small reactant mass fraction at the interface. Equations 15-18 combine to produce

$$\text{at } r = r_c \qquad s = -\frac{M_M}{xM_H}\frac{\rho^\beta}{\rho_M^\alpha} D \frac{\partial \omega_H^\beta}{\partial r} \qquad [19]$$

giving the interface velocity in terms of the reactant mass fraction at the interface. Equation 8 becomes

$$\text{at } r = r_c \qquad v_r^\beta = -\frac{M_M}{xM_H}\frac{(\rho^\beta - \rho^\alpha)}{\rho_M^\alpha} D \frac{\partial \omega_H^\beta}{\partial r} \qquad [20]$$

to be used as a boundary condition for Eq. 6.

The convection term in Eq. 9 can now be evaluated. First, we express the integration constant in Eq. 6 in terms of the particular values of r and v_r^β at the interface

$$r^2 v_r^\beta = r_c^2 v_r^\beta\Big|_{r=r_c} \qquad [21]$$

Equation 20 then provides

$$v_r^\beta = -\left(\frac{r_c}{r}\right)^2 \frac{M_M}{xM_H}\frac{(\rho^\beta - \rho^\alpha)}{\rho_M^\alpha} D \frac{\partial \omega_H^\beta}{\partial r}\Big|_{r=r_c} \qquad [22]$$

everywhere in the β-phase. The continuity equation for reactant, Eq. 9, finally becomes

$$\frac{\partial \omega_H^\beta}{\partial t} - \left(\frac{r_c}{r}\right)^2 \frac{M_M}{xM_H} \frac{(\rho^\beta - \rho^\alpha)}{\rho_M^\alpha} D \frac{\partial \omega_H^\beta}{\partial r}\bigg|_{r=r_c} \frac{\partial \omega_H^\beta}{\partial r}$$

$$= \frac{D}{r^2}\frac{\partial}{\partial r}\left(r^2 \frac{\partial \omega_H^\beta}{\partial r}\right) - \frac{R_H^\beta}{\rho^\beta} \quad [23]$$

Dimensional analysis.—The following equations define convenient dimensionless variables (time, radial position, β-phase reaction rate, a rescaled reactant mass fraction, and interface position)

$$\tau \equiv \frac{t}{t_0} \quad y \equiv \frac{r_c}{R} \quad \Re_H \equiv \frac{R_H^\beta}{R_0^\beta} \quad W \equiv \frac{\omega_H^\beta}{\omega_{HR}}$$

$$Y \equiv \frac{r - r_c}{R} = \frac{r}{R} - y \quad [24]$$

where t_0 and R_0^β are a characteristic process time and homogeneous reaction rate. The last of these effectively changes the frame of reference so that the moving α/β interface is viewed as stationary. In dimensionless form, Eq. 23 becomes

$$\frac{R^2/D}{t_0}\frac{\partial W}{\partial \tau} - \frac{\rho^\beta - \rho^\alpha}{\rho^\beta}\omega^*\left(\frac{y}{Y+y}\right)^2 \frac{\partial W}{\partial Y}\bigg|_{Y=0}$$

$$\frac{\partial W}{\partial Y} = \left(\frac{y}{Y+y}\right)^2 \frac{\partial}{\partial Y}\left[\left(\frac{Y+y}{y}\right)^2 \frac{\partial W}{\partial Y}\right] - \frac{R^2/D}{\rho^\beta/R_0^\beta}\Re_H \quad [25]$$

with

$$\omega^* \equiv \frac{M_M}{xM_H}\frac{\rho^\beta}{\rho_M^\alpha}\omega_{HR} \quad [26]$$

The initial and boundary conditions become

$$\text{at } \tau = 0 \text{ for } 0 > Y > 1 \quad W = 0 \quad [27]$$

$$\text{for } \tau > 0,\ Y = 1 - y \quad W = 1 \quad [28]$$

$$\text{for } \tau > 0,\ Y = 0 \quad W = 0 \quad [29]$$

with a dimensionless form of Eq. 19

$$\text{at } Y = 0 \quad \frac{R^2/D}{t_0}\frac{dy}{d\tau} = -\omega^*\frac{\partial W}{\partial Y} \quad [30]$$

for the α/β interface velocity. The parameter ω* is proportional to the surface mass fraction of reactant but also depends on the reaction stoichiometry and phase densities. Similar parameters appear in earlier shrinking core models.[13,16,19] Although M_M/xM_H will typically be large for low molecular weight reactants in high molecular weight solids, ω_{HR} is small, so ω* may assume arbitrary values.

For low molecular weight reactants in high molecular weight solids, $\rho^\beta - \rho^\alpha \to 0$, and so the convection term in Eq. 25 will be small compared to the other terms. In addition, we only consider situations in which the characteristic reaction time in the β-phase ρ^β/R_0^β is large compared to the diffusion time R^2/D; hence the reaction term in Eq. 25 will be eliminated. However, these assumptions are not equivalent to the PSS approximation: PSS also assumes a small diffusion time R^2/D compared to the characteristic process time t_0. The latter condition may not be met in some processes because of the small reactant diffusivity in the β-phase.

We set the characteristic process time equal to the diffusion time so that $R^2/t_0D = 1$ in Eq. 25 and 30. Retention of the transient accumulation term relaxes one of the restrictions imposed by the PSS approximation.

Mathematical analysis and solution.—In the absence of convection, the change of variables $u \equiv (Y + y)W$ converts Eq. 24 to

$$\frac{\partial u}{\partial \tau} = \frac{\partial^2 u}{\partial Y^2} \quad [31]$$

with initial and boundary conditions

$$\text{at } \tau = 0 \text{ for } 0 > Y > 1 \quad u = 0 \quad [32]$$

$$\text{for } \tau > 0,\ Y = 1 - y \quad u = 1 \quad [33]$$

$$\text{for } \tau > 0,\ Y = 0 \quad u = 0 \quad [34]$$

Differential mass balances and Fick's first law are frame indifferent equations.[20] In the frame of reference defined by the change of variables,[24] we treat the α/β interface as stationary. Consequently, we may solve Eq. 31 subject to the initial/boundary conditions 32-34 while treating y as a constant. Equation 31 has a Fourier series solution[24] in the form of

$$u(Y,\tau) = \sum_{n=1}^{\infty} T_n(\tau)\sin\left(\frac{n\pi Y}{1-y}\right) \quad [35]$$

where orthogonality of the sine function provides

$$T_n(\tau) = \frac{2}{1-y}\int_0^{1-y} u(Y',\tau)\sin\left(\frac{n\pi Y'}{1-y}\right)dY' \quad [36]$$

and y is treated as a time-independent parameter. After integrating by parts twice and using Eq. 31, Eq. 36 can be expressed as

$$T_n(\tau) = -\frac{2(-1)^n}{n\pi} - \frac{2(1-y)}{(n\pi)^2}\int_0^{1-y}\frac{\partial u(Y',\tau)}{\partial \tau}\sin\left(\frac{n\pi Y'}{1-y}\right)dY' \quad [37]$$

or, using the time derivative of Eq. 36, as

$$T_n(\tau) = -\frac{2(-1)^n}{n\pi} - \frac{2(1-y)^2}{(n\pi)^2}\frac{dT_n(\tau)}{d\tau} \quad [38]$$

Solution of this first-order ordinary differential equation with the initial condition 32 yields

$$T_n(\tau) = -\frac{2(-1)^n}{n\pi}\left[1 - \exp\left\{-\frac{n^2\pi^2\tau}{(1-y)^2}\right\}\right] \quad [39]$$

Substituting into Eq. 35 produces $u(Y, \tau)$ as

$$u(Y,\tau) = \sum_{n=1}^{\infty}\frac{2(-1)^{n-1}}{n\pi}\sin\left(\frac{n\pi Y}{1-y}\right) + \sum_{n=1}^{\infty}\frac{2(-1)^n}{n\pi}\exp\left\{-\frac{n^2\pi^2\tau}{(1-y)^2}\right\}\sin\left(\frac{n\pi Y}{1-y}\right) = \frac{Y}{1-y} + \sum_{n=1}^{\infty}\frac{2(-1)^n}{n\pi}\exp\left\{-\frac{n^2\pi^2\tau}{(1-y)^2}\right\}\sin\left(\frac{n\pi Y}{1-y}\right) \quad [40]$$

with the second form simplified using the orthogonality property of the sine function. Returning to our original dimensionless variables thus gives

$$W(Y,\tau) = \frac{Y}{(Y+y)(1-y)} + \frac{1}{(Y+y)}\sum_{n=1}^{\infty}\frac{2(-1)^n}{n\pi}\exp\left\{-\frac{n^2\pi^2\tau}{(1-y)^2}\right\}\sin\left(\frac{n\pi Y}{1-y)}\right) \quad [41]$$

From this solution, Eq. 29 for the interface velocity becomes

$$\frac{dy}{d\tau} = -\frac{\omega^*}{y(1-y)}\left[1 + 2\sum_{n=1}^{\infty}(-1)^n\exp\left\{-\frac{n^2\pi^2\tau}{(1-y)^2}\right\}\right] \quad [42]$$

Equation 42 is a nonlinear first-order differential equation that can be numerically integrated with the initial condition $y = 1$ at $\tau = 0$.

If we neglect the summation terms in Eq. 42, integration of the interface velocity yields an implicit equation

$$\tau = \frac{1}{6\omega^*}\left(1 - 3y^2 + 2y^3\right)$$

$$= \frac{1}{6\omega^*}\left[1 - 3(1 - x)^{2/3} + 2(1 - x)\right] \quad [43]$$

for the interface position y or fractional conversion $x = 1 - y^3$ as functions of time. Equation 43 is identical to the solution obtained via the PSS approximation.[13] Hence the summation terms in Eq. 42 should be viewed as transient corrections to the PSS solution.

Equation 42 is a first-order nonlinear differential equation that relates the dimensionless interface position and time. We integrated Eq. 42 numerically using the Adam-Mouton method[25] to determine $y(\tau)$. Using this, evaluation of Eq. 41 determined the dimensionless reactant mass fraction in the β-phase as a function of position and time.

Results and Discussion

Comparison of transient and PSS solutions.—Equation 42 suggests that the transient correction to the PSS solution for interface velocity may be important under some circumstances. However, the summation term in Eq. 42 must be truncated after a finite number of terms to enable numerical integration. Figure 2 shows the dimensionless interface position as a function of dimensionless time for different levels of truncation of the summation in Eq. 42. For the relatively large value of $\omega^* = 10$, we see a significant difference between the PSS solution (zero terms in the summation) and the transient solution which includes one term in the summation. This result indicates the well-known inaccuracy of the PSS approximation for large values of ω^*. The transient solution with two summation terms differs from the one-term solution, but higher numbers of summation terms make only small contributions. All subsequent results from the transient model reported here include only two terms in Eq. 42.

Predictions of the time dependence of the interface position for various values of ω^* are shown in Fig. 3. For large values of ω^*, the transient and PSS solutions differ considerably, but the difference becomes negligibly small as ω^* decreases. This result agrees with previous analyses[14,18] that indicate the validity of the PSS approximation for small values of the surface concentration of the diffusing species.

In terms of the time required to reach a specified conversion, $\tau(x)$

$$\eta(x) = \frac{\tau_{trans}(x) - \tau_{pss}(x)}{\tau_{trans}(x)} \quad [44]$$

quantifies the error of the PSS solution relative to the transient solution. Figure 4 shows this measure of error, expressed as a percentage, for various values of ω^*. As expected, the error introduced by the PSS approximation is minor for small values of ω^*, especially for conversion near unity. For values of $\omega^* > 5$, the PSS solution underestimates the time to complete conversion by more than 50%.

General characteristics of the transient solution.—Figure 3 shows that, as expected, increasing the surface mass fraction of reactant leads to a considerable decrease in the time needed to shrink the α/β interface from the particle surface to the center. Figure 5 depicts the corresponding curves for

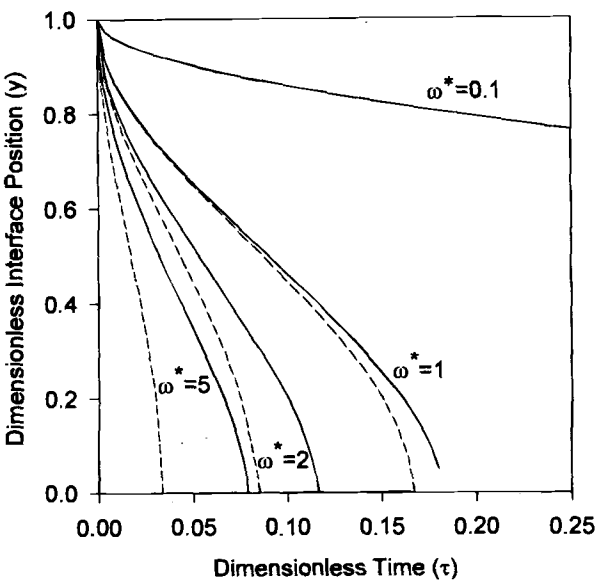

Fig. 3. Dimensionless interface position as a function of dimensionless time for various values of ω^* as predicted by the transient (solid line) and PSS (dashed line) solutions of the shrinking core model.

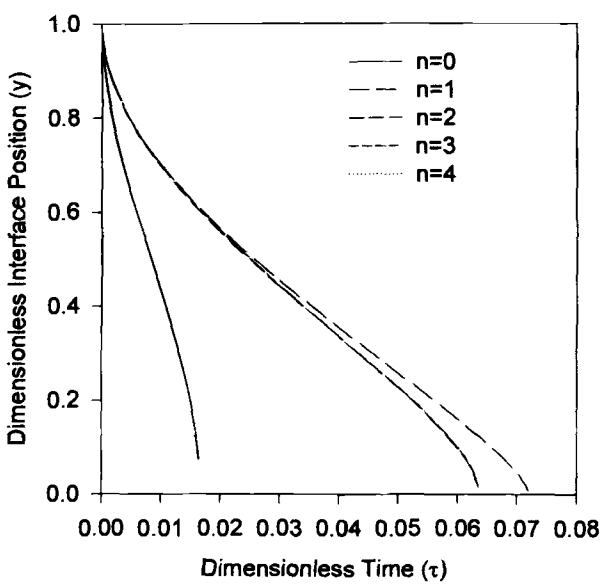

Fig. 2. Effect of truncating the summation term in Eq. 42 on the solution of the transient shrinking core model ($\omega^* = 10$).

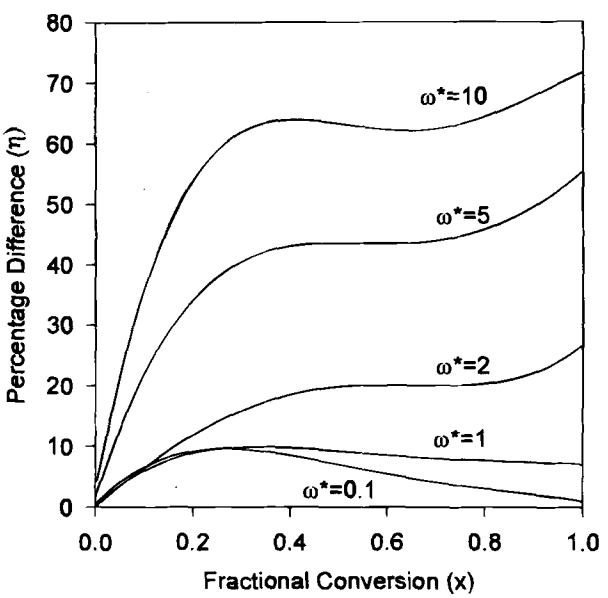

Fig. 4. Percentage by which the PSS solution underestimates the time for a given fractional conversion relative to the transient solution.

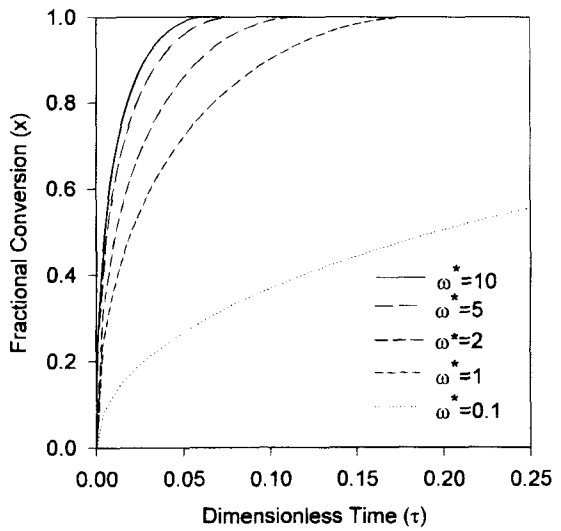

Fig. 5. Fractional conversion as a function of dimensionless time for various values of ω* as predicted by the transient solution of the shrinking core model.

the time dependence of the fractional conversion. The time needed for complete conversion of unreacted solid to product decreases with increasing values of ω*. For O(1) values of ω*, the dimensional time required for complete conversion is always less than the characteristic diffusion time (*i.e.*, $\tau_{trans}(1) < 1$) as expected for a diffusion-limited process.

Conversion profiles for various values of reactant diffusivities with fixed particle size and ω* are shown in Fig. 6. Figure 7 shows the variation of conversion with particle radius for fixed reactant diffusivity. These results and the time scaling of Eq. 24 with $t_0 = R^2/D$ show entirely expected results: increasing the reactant diffusivity or decreasing the particle radius decreases the time needed to achieve complete conversion. The conversion times indicated in Fig. 6 and 7 are typical of metal alloy particles used in hydriding applications. Small particle radii and high reactant diffusivities are clearly required if complete conversion is to occur within practical cycle times.

Figure 8 shows the distribution of free reactant inside the particle as a function of time. During the course of the reaction, the reactant mass fraction inside the particle increases monotonically with radial position. The reactant mass fraction at a fixed position increases with time. At complete conversion under these conditions, the mass fraction of free reactant near the center is about 25% of that at the particle surface. Further reactant uptake may occur due to the concentration gradient, but the amount can probably be neglected compared to that stored in the product.

Implications for hydrogen uptake by metal alloy particles.—The results of the previous section show that the transient solution of the governing equations for the shrinking core model provides a realistic description of reactant uptake by a solid particle, provided the reaction is limited to the interfacial zone between the unreacted and reacted phases. Values of the model's only parameter, ω*, determine the variation of the α/β interface position and the fractional conversion with time. When ω* is small, the solution reduces to that found under the PSS approximation. Large values of ω* lead to predictions that deviate significantly from those of the PSS solution.

The validity of the PSS approximation for hydrogen uptake by metal alloy particles is therefore determined by the magnitude of ω* defined by Eq. 26. For $LaNi_5$ with $x = 6$, we have $M_M/xM_H = 88.7$. We also assume that the densities of $LaNi_5$ and $LaNi_5H_6$ are similar so that $\rho^\beta/\rho^\alpha_M \approx 1$. The

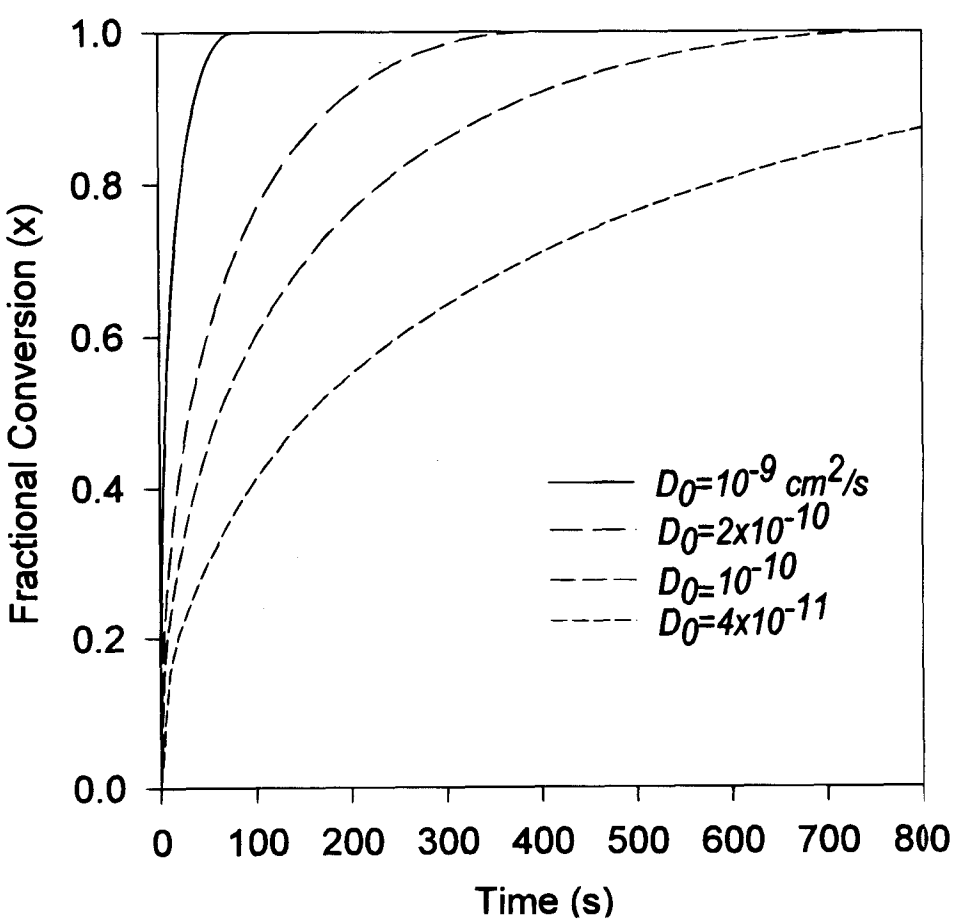

Fig. 6. Fractional conversion as a function of time for various values of the reactant diffusivity (R = 10 μm, ω* = 5).

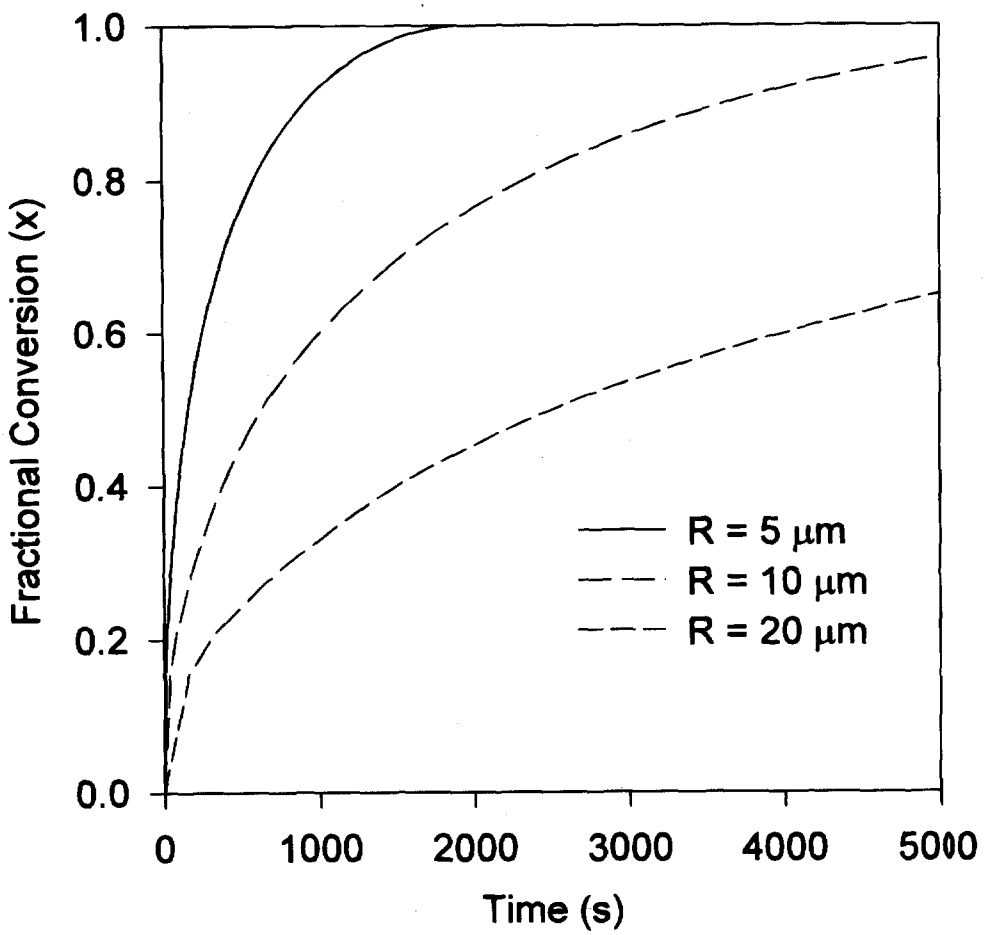

Fig. 7. Fractional conversion as a function of time for various values of the particle radius (D_0 = 10^{-10} cm^2/s, ω^* = 5).

value of ω_{HR} varies with the extent of chemisorption of H_2 on the surface and depends on the gas-phase H_2 pressure or the applied electric potential in an electrolyte solution. Unfortunately, experimental values of ω_{HR} are not available. If we suppose that $LaNi_5H_6$ may contain as much as one additional H per unit at the particle surface, then $\omega_{HR} \approx 0.00186$, and so we estimate $\omega^* \approx 0.165$ as an upper limit. Thus we conclude that the PSS approximation is reasonable for hydrogen uptake by $LaNi_5$ particles.

Extracting H diffusivities from hydriding data.—We have used a microcalorimetric technique to study the thermodynamics and kinetics of H uptake by $LaNi_5$ and related partially substituted alloys. Another publication[23] provides experimental details and more complete results. Results from one experiment are shown here to illustrate the use of the transient solution of the shrinking core model to quantify H diffusivity.

A sample of activated $LaNi_5$ alloy particles was placed in a test cell and then embedded inside a microcalorimeter (Hart Scientific Model 5024). Thermopiles placed around the test cell act as heat sinks for the energy released by the exotherm of the hydriding reaction. The temperature difference between the sample and the thermopiles is proportional to the heat flux. Admission of H_2 gas to the test cell allowed the alloy sample to adsorb H; a computer recorded the heat flux as a function of time.

The measured heat flux represents a temporal convolution of the actual hydriding reaction rate. A deconvolution procedure, discussed elsewhere,[23] transforms the measured heat flux into the reaction rate as a function of time. Assuming a constant partial molar enthalpy of the hydriding reaction,[26] the transient reaction enthalpy can be integrated and normalized with the sample's total reaction enthalpy to find the fractional hydriding conversion, x, as a function of time. The assumption of spherical particles with specified radii allows the calculation of the dimensionless α/β interface position, y, via $x = 1 - y^3$.

Figure 9 shows the α/β interface position as a function of time for a sample of $LaNi_5$ alloy exposed to H_2 gas at 7.8 atm. The solid and broken curves are fits of the experimental data using the transient and PSS solutions, respectively, assuming particle radii of 10 μm, $\omega^* = 0.165$, and using the H diffusivity as an adjustable parameter. Both the transient and PSS solutions match the data quite well and yield $D = 1.70 \times 10^{-9}$ cm^2/s.

Conclusions

The shrinking core model for reactant uptake by a solid particle assumes that the reactant-solid reaction occurs only in a narrow interfacial zone that separates unreacted

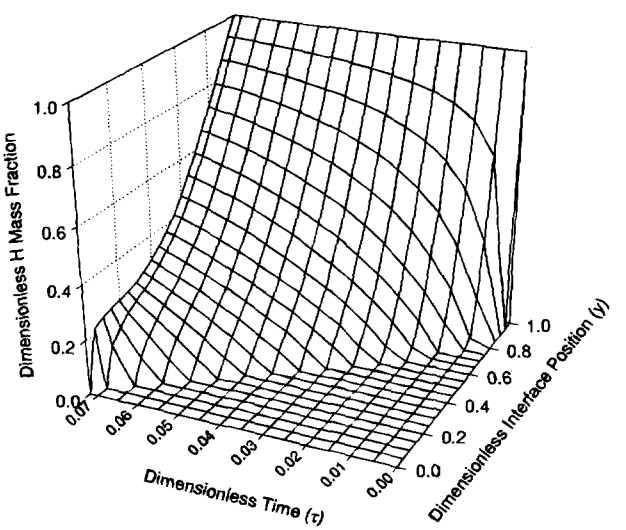

Fig. 8. Reactant mass fraction as a function of dimensionless radial position and time ($\omega^* = 5$).

solid from reacted product. We have developed a complete transport model consisting of overall and species mass balances, Fick's first law for relating the reactant mass flux to the reactant mass fraction gradient, and jump mass balances that lead to correct boundary conditions. Simplification of the governing equations in accord with dimensional analysis indicates appropriate conditions for neglecting diffusion-induced convection. The model also assumes that homogeneous reactions can be neglected in the product phase. Retention of the transient mass accumulation term in the reactant mass balance and some useful changes of variables enable a semi-analytical solution that improves upon the classic pseudo-steady state solution.

The predictions of the transient model agree with the PSS solution for small values of the surface mass fraction of entering reactant. However, under certain conditions, the PSS solution leads to an underestimation of the time required for a specified fractional conversion. Predictions of reactant diffusivity derived from the transient and PSS solutions could differ by orders of magnitude. Thus the PSS approximation must be used with caution when modeling reactant uptake by solid particles.

For the hydrogen uptake by metal alloy particles such as $LaNi_5$, a generous estimate of one "free" H atom per $LaNi_5$ unit cell leads to a small surface mass fraction of H because of the molecular weight difference between H and $LaNi_5$. Thus we expect that the PSS approximation will be valid under most conditions for H uptake by metal alloy particles.

A forthcoming publication[23] will compare predictions of the transient shrinking core model with experimental microcalorimetry data for hydrogen uptake by partially substituted $LaNi_5$. Here, we have shown that the values of H diffusivities extracted from microcalorimetry experiments depend on the value of the H mass fraction at the particle surface. Independent measurements of the surface H mass fraction are needed in order to use the model to predict H diffusivity in metal alloy particles. Alternately, independent knowledge of H diffusivity could be used to predict surface H mass fraction or, using an appropriate extension of the transient model developed here, mass transfer coefficients.

Acknowledgments

This work was sponsored by the Chemical Sciences Division, Office of Basic Energy Sciences, U.S. Department of Energy, under Contract No. DE-FG03-93ER14381. We express special thanks to Professor J. C. Slattery for his valuable suggestions. The work was carried out by one of us (W.Z.) in partial fulfillment of the requirement for the Ph.D. degree in Chemical Engineering at Texas A&M University.

Manuscript submitted Aug. 2, 1995; revised manuscript received Dec. 4, 1995.

The University of South Carolina assisted in meeting the publication costs of this article.

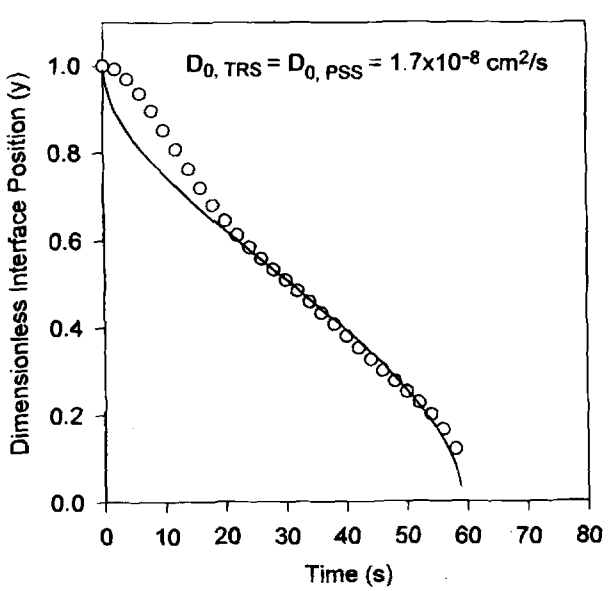

Fig. 9. Dimensionless interface position as a function of time for $LaNi_5$ alloy particles being hydrided under H_2 gas at 7.8 atm. The circles are experimental data. The solid and broken curves are the predictions of the transient and PSS solutions, respectively, assuming particle radii of 10 μm and $\omega^* = 0.165$.

LIST OF SYMBOLS

C	integration constant
D	reactant diffusivity, m^2/s
e	electron
M	molecular weight, kg/mol
n	index
n_H	reactant mass flux, kg/m^2s
r	radial position, m
r_c	radial position of the α/β interface, m
R	metal alloy particle radius, m
R_0^β	characteristic rate of reactant consumption in the β-phase, kg/m^3 s
R_H^β	rate of reactant consumption in the β-phase, kg/m^3 s
R_H^σ	rate of reactant consumption at the α/β interface, kg/m^2 s
R_M^σ	rate of M consumption at the α/β interface, kg/m^2 s
s	velocity of the α/β interface, m/s
t	time, s
t_0	characteristic process time, s
T_n	coefficient in Fourier sine solution
u	dependent variable in Eq. 30
v_r	mass-average radial velocity, m/s
W	rescaled reactant mass fraction, $\omega_H^\beta/\omega_{HR}$
x	number of reactant atoms per unit of product; fractional conversion
y	dimensionless radial position of the α/β interface
Y	dimensionless radial position, $(r - r_c)/R$

Greek

α	unreacted solid phase
β	reacted product phase
η	relative error
ρ	mass density, kg/m^3
σ	interfacial
τ	dimensionless time, t/t_0
ω	mass fraction
ω*	dimensionless surface mass fraction of reactant, defined in Eq. 25

Subscripts and superscripts

ads	adsorbed
c	at the α/β interface
H	reactant; hydrogen
H0	initial value for reactant
HR	surface value for reactant
i	generic phase
M	solid; metal alloy
PSS	pseudo-steady state
r	radial component
trans	transient solution

REFERENCES

1. J. H. N. Van Vucht, F. A. Kuijpers, and H. C. A. Buruning, *Philips Res. Repts.*, **25,** 133 (1970).
2. F. E. Lynch, *J. Less-Common Met.*, **172,** 943 (1991).
3. W. Zhang, Ph.D. Thesis, Texas A&M University, College Park, TX (1995).
4. O. Boser, *J. Less-Common Met.*, **46,** 91 (1976).
5. C. N. Park and J. Y. Lee, *ibid.*, **83,** 39 (1982).
6. A. J. Goudy, D. G. Stokes, and J. A. Gazzillo, *ibid.*, **91,** 149 (1983).
7. W. Zhang, J. Cimato, and A. J. Goudy, *J. Alloys Compd.*, **201,** 175 (1992).
8. X.-L. Wang and S. Suda, *Int. J. Hydrogen Energy,* **18,** 139 (1992).
9. D. Richter, R. Hempelmann, and R. C. Bowman, Jr., in *Topics in Applied Physics,* Vol. 67, S. Schlapbach, Editor, Springer-Verlag, Berlin (1992).
10. R. C. Bowman, Jr., B. D. Craft, A. Attalla, M. H.

Mendelsohn, and D. M. Gruen, *J. Less-Common Met.*, **73,** 227 (1980).
11. F. E. Spada, H. Oesterreicher, R. C. Bowman, Jr., and B. D. Craft, *Phys. Rev.*, **B30,** 4909 (1984).
12. S. Yagi and D. Kunii, *Chem. Eng. Sci.*, **16,** 634 (1961).
13. K. B. Bischoff, *ibid.*, **18,** 711 (1963).
14. J. R. Bowen, *ibid.*, **20,** 712 (1965).
15. K. B. Bischoff, *ibid.*, **20,** 783 (1965).
16. T. G. Theofanous and H. C. Lim, *ibid.*, **26,** 1297 (1970).
17. N. Lindman and D. Simonsson, *ibid.*, **34,** 31 (1979).
18. G. F. Carey and P. Murray, *ibid.*, **44,** 979 (1989).
19. P. Carabin and D. Berk, *ibid.*, **47,** 2499 (1992).
20. J. C. Slattery, *Momentum, Energy, and Mass Transfer in Continua*, 2nd ed., Robert E. Krieger Publishing, Huntington, NY (1981).
21. J. Y. Lee, S. M. Byun, C. N. Park, and J. K. Park, *J. Less-Common Met.*, **87,** 149 (1982).
22. J. J. Reilly, in *Proceedings of the Symposium on Hydrogen Storage Materials, Batteries, and Electrochemistry*, D. A. Corrigan and S. Srinivasan, Editors, PV 92-5, p. 24, The Electrochemical Society Proceedings Series, Pennington, NJ (1992).
23. W. Zhang, M. P. S. Kumar, A. Visintin, S. Srinivasan, H. J. Ploehn, *J. Alloys Compd.*, (1995).
24. N. S. Koshlyaakov, M. M. Smirnov, and E. B. Gliner, *Differenitial Equations of Mathematical Physics*, North-Holland, Amsterdam (1964).
25. C. W. Gear, *Numerical Initial-Value Problems in Ordinary Differential Equations*, Prentice-Hall, Englewood Cliffs, NJ (1971).
26. T. B. Flanagan, W. Luo, and J. D. Clewley, in *Hydrogen Storage Materials, Batteries, and Electrochemistry*, D. A. Corrigan and S. Srinivasan, Editors, PV 92-5, p. 46, The Electrochemical Society Proceedings Series, Pennington, NJ (1992).

A Novel Electrolyte Solvent for Rechargeable Lithium and Lithium-Ion Batteries

S. S. Zhang and C. A. Angell*

Department of Chemistry, Arizona State University, Tempe, Arizona 85287-1604, USA

ABSTRACT

We describe a new type of electrolyte solvent which provides remarkable improvement in properties of electrolyte systems containing it. These solvents contain acidic boron atoms, in most cases linked into heterocycles by reaction of boric acid, or oxide, with glycols. Nicknamed BEG solvents (for boric acid esters of glycol), these show great propensity for dissolving salts, stabilizing alkali metals against corrosion, and in some cases, stabilizing other solvents (particularly alkene carbonates), against anodic decomposition. In the most favorable case so far, the 1,3 propylene glycol boric acid ester (BEG-1) which contains two linked borate groups, the mixed solvent formed by mixing 1 part BEG-1 with two parts ethylene carbonate provides an electrochemical stability window in excess of 5.8 V (cf. 4.5 V for ethylene carbonate alone with the same salt), an ambient temperature conductivity of 1.7×10^{-3} S cm^{-1} with 1 *m* $LiClO_4$, and enduring stability against metallic Li, which remains shiny on prolonged (days) immersion at 100°C. We present data on various electrolyte solutions containing these components and then show their utility in devices by rubberizing them with polymers and constructing voltaic cells $Li/LiMn_2O_4$ and $C/LiMn_2O_4$, which show excellent charge/discharge characteristics and cyclability.

Introduction

Many nonaqueous electrolytes and polymer gel electrolytes, compromising polar organic solvents and their mixtures and having ambient ionic conductivities above 10^{-3} S/cm, have been developed for use with rechargeable lithium and carbonaceous anode lithium-ion batteries. Unfortunately, metallic lithium reacts with almost all organic solvents to form a low-conductivity passivation layer on the surface of the lithium, and repeated cycling frequently produces dendritic deposits which eventually short-circuit the batteries. Batteries using inorganic chloride electrolytes, such as $Li/SOCl_2$ and Li/SO_2Cl_2 batteries, suffer from voltage delay problems due to the formation of a polycrystalline LiCl passivation layer on the lithium surface. As a result of such electrolyte problems, the development of rechargeable lithium batteries has been greatly inhibited.

A wide variety of approaches has been used in attempts to improve lithium deposition morphology and to increase lithium cycling efficiency, with little success so far. Typical examples have been the use of organic or inorganic additives,[1-12] introduction of new salts,[13-17] Li alloys,[18-20] and finally, the lithium-free carbon anode.[21-24] Even in the case of carbonaceous anode lithium-ion batteries, in which the use of metal lithium is completely avoided, there remains an electrolyte problem limiting development. It is found that the common electrolyte solvents, such as propylene carbonate (PC) and ethylene carbonate (EC), easily cointercalate into carbon layers and decompose on the surface of fresh carbon particles (probably because of the electrocatalytic nature of fresh carbon structure). This leads to an irreversibility of the first cycle, requiring extra lithium-rich cathode material ($LiCoO_2$, $LiNiO_2$, or $LiMnO_2$) to be included in the cells in order to compensate for the consumption in the initial irreversible cycle. To minimize this irreversibility of initial lithium intercalation, the use of co-solvents[25-27] and the modification of carbonaceous structure[28-31] have been investigated. However, none of the above-mentioned methods is suitable for both lithium anode and carbon anode. Thus, a great need exists for new solvents and co-solvents with special stability in the presence of lithium metal. This in effect requires an ability of the solvent to react with metallic lithium in a benign way, *i.e.*, so as to generate a stable Li^+-conducting, nonpropagating film on the lithium surface. We report here on a class of molecular substance which appears to behave in this desirable manner and has remarkable stabilizing effects on co-solvents at positive potentials as well.

Our original motivation in this work was to find a molecular liquid which would dissolve salts by solvating the anions in order that the alkali metal transport number could become more favorable. To this end, we prepared initially the boron analog of propylene carbonate, viz.

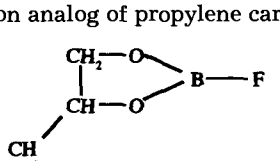

with the idea that the under-coordinated boron would seek a fourth ligand from the salt anion. Indeed, this liquid proves to be an excellent solvent for salts. However, it is a much more viscous liquid than PC, presumably due to intermolecular interactions of the type

* Electrochemical Society Active Member.